Thermal Dynamical Identification of Light-Emitting Diodes by Step-Based Realization and Convex Optimization

Daniel N. Miller, *Student Member, IEEE*, Jeff Hulett, James McLaughlin, and Raymond A. de Callafon, *Member, IEEE*

***Abstract*— A new method for modeling the thermal response of semiconductor devices such as light-emitting diodes (LEDs) from temperature measurements is presented. The method uses a realization-theoretic approach to identification combined with convex optimization methods. Linear matrix inequalities are constructed to guarantee that the identified discrete-time model has strictly real eigenvalues between 0 and 1, so that, when converted to continuous time, the model will have strictly real time constants. Additional optional time-domain constraints are developed to guarantee a predetermined steady-state value, guarantee no undershoot or overshoot in the transient response, and/or guarantee a positive time-constant spectrum. The method is applied to the thermal response of a high-power LED. Temperature measurements of the semiconductor device are used to model the time constants of the thermal response and characterize the relative contribution of each time constant to temperature increase. Experiments indicate how the proposed method can be used to detect thermal defects. It is shown that models with five time constants can model the thermal effects of the LEDs used with high accuracy. The proposed method is applicable to larger order systems with multiple simultaneous temperature measurements.**

***Index Terms*— Convex optimization, light-emitting diodes, linear-matrix inequalities, realization theory, step response, system identification, time-constant spectrum.**

NOMENCLATURE

DIMENSIONS

n	Dimension of state vector/order of linear model.
n_y	Dimension of step-response signal.
P	Columns in $H, \overline{H}, Y, \overline{Y}$.
r	Block-rows in $H, \overline{H}, Y, \overline{Y}$.

LMI REGIONS

f_*	Describing function of LMI region *.
P	Region of complex plane such that Re(z) $\geq \delta_p$.
R	Region of complex plane such that Im(z) $\leq \delta_r$.
S	Region of complex plane inside circle of radius 1–δ_p.

SIGNALS AND PARAMETERS

(A_c, B_c, C_c)	Continuous-time state-space parameters.
(A_d, B_d, C_d)	Discrete-time state-space parameters.
$\mathcal{C}$	Extended controllability matrix.
k	Discrete-time sample index.
$\Lambda_c, \lambda_c^{(i)}$	Eigenvalues, ith eigenvalue of A_c.
$\lambda_d^{(i)}$	ith eigenvalue of A_d.
$\mathcal{O}$	Extended observability matrix.
R_i	Relative contribution of ith continuous-time time constant.
t	Continuous time variable.
τ_i	ith continuous-time time constant of linear model.
T_s	Sampling time of step-response measurement.
$V_c, v_c^{(i)}$	Left eigenvectors, ith left eigenvector of A_c.
$x_c(t)$	Continuous-time state vector.
$x_d(k)$	Discrete-time state vector.
$y(t)$	Continuous-time step response signal.
$y_d(k)$	Discrete-time step-response signal.

DATA MATRICES

$*$	Block-matrix of data (*) shifted up by a block-row or left by a block-column.
H	Block-Hankel matrix of discrete-time Markov parameters.
M	Matrix of step-response data with repeated columns.
$\mathbf{\Omega}$	Estimate of HU_p.
$\overline{\mathbf{\Omega}}$	Estimate of $\overline{H}U_p$.
ϕ	Regressor for B_d.
T	Block-Toeplitz matrix of discrete-time Markov parameters.
U_f	Matrix of 1 everywhere.
U_n, Σ_n, V_n^T	First n left singular vectors, singular values, and right singular vectors, of $\mathbf{\Omega}$.
U_p	Upper-triangular matrix of 1.

Manuscript received April 23, 2012; revised September 1, 2012; accepted November 9, 2012. Date of publication January 9, 2013; date of current version May 29, 2013. Recommended for publication by Associate Editor M. K. Iyengar upon evaluation of reviewers' comments.

D. N. Miller and R. A. de Callafon are with Jacobs School of Engineering, University of California San Diego, La Jolla, CA 92093 USA (e-mail: d6miller@ucsd.edu; callafon@ucsd.edu).

J. Hulett and J. McLaughlin are with Vektrex Corporation, San Diego, CA 92121 USA (e-mail: jhulett@vektrex.com; jrmclaugh@vektrex.com).

Color versions of one or more of the figures in this paper are available online at http://ieeexplore.ieee.org.

Digital Object Identifier 10.1109/TCPMT.2012.2229464

U_s, Σ_s, V_s^T Remaining s left singular vectors, singular values, and right singular vectors, of Ω.
ξ Column-vector of samples of $y_d(t)$.
Y Block-Hankel matrix of step-response measurements.

I. Introduction

EXPERIMENTAL analysis of thermal transients plays an important role in the model validation and failure detection of integrated circuits. Such thermal responses are typically modeled as resistor–capacitor networks, with the various resistances and capacitances derived from known thermal properties of the materials. These networks can be created from numerical simulations or from experimental measurements.

One popular framework for analyzing the thermal response of packaged electronics is that of the time-constant spectrum, developed by Székely. This framework replaces the finite-dimensioned resistor–capacitor networks with an infinitely long network to form a continuum of time constants as a function of a logarithmic time variable. The step response is formulated in terms of the convolution of an analytic function (the spectrum) with a unit exponential rise. The original method consists of a transformation to a logarithmic time variable, followed by a differentiation and a deconvolution to generate a nonparametric estimate of the spectrum function [1]. Relationships between the impedance of a circuit and its time-constant spectrum were later derived in [2] and [3].

While an automatically generated graph of the time-constant spectrum provides an immediate and intuitive interpretation of the various transient artifacts of the step response, an additional curve-fitting or discretization procedure is required in order to define the spectrum with a finite number of parameters. Hence estimating the time-constant spectrum function in this manner is essentially a nonparametric identification procedure, akin to measuring the frequency response function of a linear system. Also, the calculation of the spectrum requires differentiation of the measured step response followed by deconvolution with a low-pass filter, both of which reduce the signal-to-noise ratio of the data.

In [4], a weighted-discretization method was proposed that reduced the number of observed time constants based on equidistant spacing along the logarithmic time axis, but the number of time constants derived was between 60 and 120. In [5], filtering techniques were developed to address loss of resolution in the time-constant spectrum when two known constants are relatively close to each other. In [6], the introduction of material properties was proposed to correct for model discrepancies due to parasitic heat loss.

Other approaches to modeling the thermal response from experimental data include applying a constrained nonlinear least-squares curve-fitting method to minimize the root-mean-square error for a continuous-time parameterization of a step response, developed in [7]. The method was applied to multivariable data, in which the effects of a step on each input were measured for multiple output signals, forming a step-response matrix of transients. The method requires careful model selection beforehand and an initial guess as to the value of the step-response time constants to avoid becoming trapped in local minima. Genetic algorithms were applied to a similar problem in [8].

In [9], automatic model reduction for deterministic electrothermal models of semiconductor devices was studied. A balanced-truncation method for reducing the order of linear systems, which shares some qualities with the identification method to be presented in this paper, was shown to be an effective way of reducing model order but was concluded to be computationally unattractive due to the extremely large order of the deterministic models. The application of model reduction to systems identified from simulated or measured data was not studied.

In this paper, we propose a novel method of parametrically identifying a linear finite-order step-response model from discrete-time measured data, which is a significant departure from existing methods in the literature. It is rooted in the realization-theoretic framework of linear systems established by Kalman in the 1960s, and in particular, the Ho–Kalman algorithm [10], which uses a block-Hankel matrix of impulse response coefficients to compute a state-space realization of a linear time-invariant system. The Ho–Kalman algorithm was later improved by Zeiger and McEwen [11] and Kung [12] to use the singular-value decomposition (SVD) to factor the block-Hankel matrix, which resulted in a certain type of optimality in a model-reduction framework [13].

Helmont *et al.* [14] derived a little known and underappreciated extension of the Ho–Kalman algorithm to step-response measurements was for the purpose of developing an optimal control law for a coal-fired Benson boiler. This step-based realization (SBR) method was later reintroduced in a subspace identification framework in [15]. The SBR provides an exact minimal-order model of a linear time-invariant system when applied to deterministic data and very good estimates when applied to noise-corrupted data.

This paper extends the SBR to include convex constraints, transforming the SBR into a semidefinite program. This new method has a number of key advantages: 1) no differentiation of the step-response is required, allowing for application to measurements with low signal-to-noise ratios; 2) the model order is chosen during the identification procedure, and no prior assumptions must be made regarding the number or location of time constants; 3) the relationship of the algorithm to model-reduction procedures inherently produces low-order models; 4) the step response can be possibly vector-valued, although multivariable measurements do not necessarily increase the system order; 5) the time constants of the model are guaranteed to be real and stable; 6) the steady-state value of the step response may optionally be constrained during identification; and 7) the method involves no nonconvex optimization. The calculation of the model parameters requires only standard operations of linear algebra, a linear programming problem, and a quadratic programming problem, for which robust numerical tools that guarantee a solution are freely available.

The rest of this paper is structured as follows. Section II formulates the identification problem. Constraints on a discrete-time state-space model are constructed to guarantee that the

model has an equivalent representation as a time-constant series model. Section III presents the unconstrained SBR method, which identifies discrete-time linear systems from measured step responses. Section IV restates the constraints given in Section II in terms of linear matrix inequalities (LMIs) that may be used to form a constrained convex optimization problem. Section V applies the method to an experimentally measured thermal response of an light-emitting diodes (LED).

In this paper, $>$ and $<$ represent elementwise greater-than and less-than, respectively, when applied to vectors or matrices, and $\succ$ and $\prec$ represent positive definiteness and negative definiteness. Nonstrict inequalities should be read similarly.

II. Problem Formulation

We begin with the assumption that the true noisefree step response of the thermal system has the form

$$y(t) = \sum_{i=1}^{n} R_i(1 - e^{-t/\tau_i}) \tag{1}$$

where $y(t) \in \mathbb{R}^{n_y}$ is a possibly vector-valued signal, τ_i are the time constants of the response, and $R_i \in \mathbb{R}^{n_y \times 1}$ are the relative contribution of each time constant to the total response. The pairs $(\tau_i,\ R_i)$ form the time-constant spectrum. Such models may also be represented as canonical forms of resister–capacitor networks [2], though we will focus on identification of the parameters τ_i and R_i in this paper.

We assume that the response is nonoscillatory to avoid a possible overshoot in temperature, which would imply the temperature might exceed the steady-state value and possibly violate the laws of thermodynamics. This requires that τ_i be real, or

$$\mathrm{Im}(\tau_i) = 0. \tag{2}$$

Allowing for complex τ_i would also require that the time constants come in complex conjugate pairs; otherwise, $y(t)$ will not be real-valued. We also assume that the system is stable so that the step response is bounded, and thus

$$\tau_i > 0. \tag{3}$$

An alternative step-response model proposed by Székely defines the time-constant spectrum as an analytical function $R(\tau)$ derived from the convergence of the $(R_i,\ \tau_i)$ pairs as $\tau_{i+1} - \tau_i \to 0$. The step response is then given by the convolution integral

$$y(t) = \int_{-\infty}^{\infty} R(\zeta)(1 - \exp(-t/e^{\zeta})d\zeta \tag{4}$$

where ζ is a dummy variable in logarithmic time. The two definitions, though conceptually similar, are not interchangeable, since the integral (4) is always 0 if $R(\tau)$ is bounded and nonzero for a finite number of τ, which is the case for (1). In this paper, we focus exclusively on identifying parametric models of the form (1).

A. Discretization of the Step-Response Model

Because (1) is a finite-dimensional linear time-invariant system, it has an alternative state-space representation

$$\begin{aligned} \dot{x}_c(t) &= A_c x_c(t) + B_c \\ y(t) &= C_c x_c(t) \end{aligned} \tag{5}$$

in which $x_c(t) \in \mathbb{R}^n$ is the state of the system, and $A_c \in \mathbb{R}^{n \times n}$, $B_c \in \mathbb{R}^{n \times 1}$ and $C_c \in \mathbb{R}^{n_y \times n}$ are the state-space parameters. The initial state is $x_c(0) = 0$, and the subscript c denotes that the parameters are from a continuous-time model. We assume that (5) is controllable, observable, and minimal, so that the state dimension n cannot be reduced. These assumptions are consistent with (1). The step response $y(t)$ may be expressed in terms of (5) as

$$y(t) = C_c A_c^{-1}(e^{A_c t} - I)B_c \tag{6}$$

where $e^{(\cdot)}$ is the matrix exponential.

The parameterization $(A_c,\ B_c,\ C_c)$ is unique only with respect to a specific state basis, but the eigenvalues of A_c are invariant. Suppose A_c has the eigenvalue decomposition

$$A_c = V_c \Lambda_c V_c^{-1}.$$

If $\lambda_c^{(i)}$ is an eigenvalue of A_c, and $v_c^{(i)}$ its associated eigenvector, then (1) may be derived from (5) via the identities

$$\tau_i = -1/\lambda_c^{(i)} \tag{7}$$

$$R_i = \tau_i C_c M_c^{(i)} B_c \tag{8}$$

where $M_c^{(i)}$ is the rank-1 matrix

$$M_c^{(i)} = v_c^{(i)}(V_c^{-1})_{(k,:)} \in \mathbb{R}^{n \times n} \tag{9}$$

in which "MATLAB-style" indexing notation has been used in the subscript. Note that $M_c^{(i)}$ is strictly real because τ_i are real.

Suppose $y(t)$ is measured in discrete time with a sampling rate of T_s. Let $y_d(k) \triangleq y(kT_s)$ be the discrete-time step-response measurement, assuming a zero-order hold for each sample. Letting the subscript d denote discrete-time state-space parameters, the discrete-time equivalent of (5) is then

$$\begin{aligned} x_d(k+1) &= A_d x_d(k) + B_d \\ y_d(k) &= C_d x_d(k) \end{aligned} \tag{10}$$

and the equivalent of (6) is

$$y_d(k) = \begin{cases} 0, & k = 0 \\ \displaystyle\sum_{l=0}^{k} C_d A_d^{l-1} B_d, & k > 0 \end{cases} \tag{11}$$

where

$$A_d = e^{A_c T_s}, \quad B_d = A_c^{-1}(A_d - I)B_c, \quad C_d = C_c.$$

The parameters $C_d A_d^k B_d$ are the discrete-time impulse response coefficients, also known as the system Markov parameters.

If the eigenvalues of A_c are strictly real, then they will have a unique equivalent in the complex plane regardless of the sampling frequency. This is because each eigenvalue introduces an exponential lag to the step response that decays

asymptotically, and so it is theoretically impossible for its effects to be hidden by aliasing. It is possible, however, for its effects to be hidden by noise, and so it is generally desirable that the eigenvalues be less than half the sampling frequency or, equivalently, that the time constants be at least twice the sampling time.

Because our data is measured in discrete time, we first identify the parameters (A_d, B_d, C_d), convert them to continuous time to find (A_c, B_c, C_c), and finally use (7) and (8) to convert the model to the form of (1).

III. Step-Based Realization

The following outlines the steps of the SBR method. Readers familiar with subspace identification methods will notice similarities with the SBR method, as both share a common ancestor in the Ho–Kalman realization algorithm. Standard subspace identification techniques are not applicable to measured step response data because the input is nonstationary. (See [16] for details regarding subspace identification methods and persistence of excitation.)

A. Formulation of the Data-Matrix Equations

Let H be a block-Hankel matrix of discrete-time Markov parameters with r block rows and p columns

$$H = \begin{bmatrix} C_dB_d & C_dA_dB_d & \cdots & C_dA_d^{p-1}B_d \\ C_dA_dB_d & C_dA_d^2B_d & \cdots & C_dA_d^pB_d \\ \vdots & \vdots & & \vdots \\ C_dA_d^{r-1}B_d & C_dA_d^rB & \cdots & C_dA_d^{r+p-2}B_d \end{bmatrix} \tag{12}$$

and let $\overline{H}$ be H shifted by one block-row or block-column to form

$$\overline{H} = \begin{bmatrix} C_dA_dB_d & C_dA_d^2B_d & \cdots & C_dA_d^pB_d \\ C_dA_d^2B_d & C_dA_d^3B_d & \cdots & C_dA_d^{p+1}B_d \\ \vdots & \vdots & & \vdots \\ C_dA_d^rB_d & C_dA_d^{r+1}B_d & \cdots & C_dA_d^{r+p-1}B_d \end{bmatrix}.$$

Assume p and r are large enough so that $p > n$ and $r > n$. The block-Hankel matrices H and $\overline{H}$ may be written in terms of the extended observability matrix $\mathcal{O}$ and the extended controllability matrix $\mathcal{C}$, where

$$\mathcal{O} = \begin{bmatrix} C_d \\ C_dA_d \\ \vdots \\ C_dA_d^{r-1} \end{bmatrix}, \qquad \mathcal{C} = \begin{bmatrix} B_d & A_dB_d & \cdots & A_d^{p-1}B_d \end{bmatrix}$$

so that

$$H = \mathcal{O}\mathcal{C}, \qquad \overline{H} = \mathcal{O}A_d\mathcal{C}.$$

Let Y be a block-Hankel matrix of step-response measurements $y_d(k)$ with r block rows and p columns starting at $k = 1$

$$Y = \begin{bmatrix} y_d(1) & y_d(2) & \cdots & y_d(p) \\ y_d(2) & y_d(3) & \cdots & y_d(p+1) \\ \vdots & \vdots & & \vdots \\ y_d(r) & y_d(r+1) & \cdots & y_d(p+r-1) \end{bmatrix}.$$

This matrix may be expressed in terms of H and a block-Toeplitz convolution matrix

$$T = \begin{bmatrix} 0 & & & \cdots & 0 \\ C_dB_d & 0 & & & \vdots \\ C_dA_dB_d & C_dB_d & \ddots & & \\ \vdots & \vdots & \ddots & 0 & \\ C_dA_d^{r-2}B_d & C_dA_d^{r-3}B_d & \cdots & C_dB_d & 0 \end{bmatrix}$$

which satisfy the data-matrix equation

$$Y = HU_p + TU_f = \mathcal{O}\mathcal{C}U_p + T_U f \tag{13}$$

in which U_p and U_f represent "past" and "future" input, respectively. To understand this terminology, note that in the case of measuring arbitrary input–output data, if a column of Y starts with some sample $y_d(k_0)$, then the corresponding column of U_p contains input for $k < k_0$, and the corresponding column of U_f contains input for $k \geq k_0$.

For a step response, the input to the system is 0 for all $k < 0$ and 1 for all $k \geq 0$, so U_p is an upper-triangular matrix with all elements equal to 1 on and above the diagonal, and U_f is a matrix of 1 everywhere

$$U_p = \begin{bmatrix} 1 & 1 & \cdots & 1 \\ & 1 & \cdots & 1 \\ \vdots & & \ddots & \vdots \\ 0 & \cdots & & 1 \end{bmatrix}, \qquad U_f = \begin{bmatrix} 1 & 1 & \cdots & 1 \\ 1 & 1 & \cdots & 1 \\ \vdots & \vdots & & \vdots \\ 1 & 1 & \cdots & 1 \end{bmatrix}.$$

Let $\overline{Y}$ be a block-Hankel matrix of step-response measurements $y_d(k)$, also with r block rows and p columns, but shifted forward by one sample

$$\overline{Y} = \begin{bmatrix} y_d(2) & y_d(3) & \cdots & y_d(p+1) \\ y_d(3) & y_d(4) & \cdots & y_d(p+2) \\ \vdots & \vdots & & \vdots \\ y_d(r+1) & y_d(r+2) & \cdots & y_d(p+r) \end{bmatrix}.$$

This can be expressed in terms of $\overline{H}$ and a forward-shifted block-Toeplitz matrix

$$\overline{T} = \begin{bmatrix} C_dB_d & 0 & & \cdots & 0 \\ C_dA_dB_d & C_dB_d & \ddots & & \vdots \\ \vdots & \vdots & \ddots & 0 & \\ C_dA_d^{r-2}B_d & C_dA_d^{r-3}B_d & \cdots & C_dB_d & 0 \\ C_dA_d^{r-1}B_d & C_dA_d^{r-2}B_d & \cdots & C_dA_dB_d & C_dB_d \end{bmatrix}$$

to form a forward-shifted data-matrix equation

$$\overline{Y} = \overline{H}U_p + \overline{T}U_f = \mathcal{O}A_d\mathcal{C} + \overline{T}U_f \tag{14}$$

in which the matrices U_p and U_f are unchanged.

Our goal is to estimate A_d using the shifting property of (13) and (14). First, however, we must isolate the system Hankel matrices H and $\overline{H}$ by removing the products TU_f and $\overline{T}U_f$.

B. Isolation of the System Hankel Matrix

Because T and $\overline{T}$ are multiplied on the right by a matrix in which all entries are 1, the products TU_f and $\overline{T}U_f$ are column-identical matrices in which each column is a sum of all the columns of T and $\overline{T}$, respectively. Hence

$$TU_f = \begin{bmatrix} 0 & 0 & \cdots \\ C_d B_d & C_d B_d & \cdots \\ \vdots & \vdots & \\ \sum_{l=0}^{r-2} C_d A_d^{l-1} B_d & \sum_{l=0}^{r-2} C_d A_d^{l-1} B_d & \cdots \end{bmatrix}$$

and

$$\overline{T}U_f = \begin{bmatrix} C_d B_d & C_d B_d & \cdots \\ C_d(A_d + I)B_d & C_d(A_d + I)B_d & \cdots \\ \vdots & \vdots & \\ \sum_{l=0}^{r-1} C_d A_d^{l-1} B_d & \sum_{l=0}^{r-1} C_d A_d^{l-1} B_d & \cdots \end{bmatrix}.$$

In the noisefree case, these matrices are equal to matrices of output data

$$M = \begin{bmatrix} y_d(0) & y_d(0) & \cdots & y_d(0) \\ y_d(1) & y_d(1) & \cdots & y_d(1) \\ \vdots & \vdots & & \vdots \\ y_d(r-1) & y_d(r-1) & \cdots & y_d(r-1) \end{bmatrix}$$

and

$$\overline{M} = \begin{bmatrix} y_d(1) & y_d(1) & \cdots & y_d(1) \\ y_d(2) & y_d(2) & \cdots & y_d(2) \\ \vdots & \vdots & & \vdots \\ y_d(r) & y_d(r) & \cdots & y_d(r) \end{bmatrix}.$$

For noise-corrupted measurements, this will not be true exactly, but we may still use the approximations $M \approx TU_f$ and $\overline{M} \approx \overline{T}U_f$ to form the estimates

$$\begin{aligned} \Omega &= Y - M = HU_p + E \approx \mathcal{O}\mathcal{C} \\ \overline{\Omega} &= Y - \overline{M} = \overline{H}U_p + \overline{E} \approx \mathcal{O}A_d\mathcal{C}U_p \end{aligned} \tag{15}$$

where E and $\overline{E}$ are error terms on the estimates of HU_p and $\overline{H}U_p$, respectively, due to the noise on $y_d(k)$.

We could multiply Ω and $\overline{\Omega}$ by the inverse of U_p to try and estimate H and $\overline{H}$ directly, but this has the effect of numerically differentiating the output, thereby amplifying high-frequency noise on the measurements. (This may be seen by computing the inverse of U_p.) Instead, we use the SVD of Ω to estimate $\mathcal{O}$ and $\mathcal{C}U_p$.

C. Computing the System Estimate

Because the system is controllable and observable, $\text{rank}(\mathcal{C}) = \text{rank}(\mathcal{O}) = n$, which implies that $\text{rank}(HU_p) = \text{rank}(\overline{H}U_p) = n$, since U_p is of full rank. If the output measurements are noisefree, then $\Omega = HU_p$, implying $\text{rank}(\Omega) = n$. Because in reality the output measurements contain nondeterministic components, Ω will have full rank, and we must construct a rank-n estimate of Ω instead.

Let Ω have the SVD

$$\Omega = U\Sigma V^T = \begin{bmatrix} U_n & U_s \end{bmatrix} \begin{bmatrix} \Sigma_n & 0 \\ 0 & \Sigma_s \end{bmatrix} \begin{bmatrix} V_n^T \\ V_s^T \end{bmatrix} \tag{16}$$

in which the matrices U and V are orthogonal, Σ is a diagonal matrix of nonnegative singular values in descending order

$$\cdots \geq \sigma_{i-1} \geq \sigma_i \geq \sigma_{i+1} \geq \cdots$$

U_n has the first n columns of U, V_n^T has the first n rows of V^T, and Σ_n has the first n rows and first n columns of Σ.

If $\text{rank}(\Omega) = n$, then Ω would have only n nonzero singular values so that $\Sigma_s = 0$. If the system order n is known beforehand, a rank-n approximation Ω_n of Ω for which

$$\Omega_n = \arg\min \text{rank}(\Omega_n) = n \, ||\Omega_n - \Omega||_2$$

is given by [17] as

$$\Omega_n = U_n \Sigma_n V_n^T. \tag{17}$$

Any rank-preserving factorization of Ω_n with valid dimensions may be used to estimate $\mathcal{O}$ and $\mathcal{C}U_p$ in the deterministic case. In the nondeterministic case, however, a numerically attractive choice is

$$\hat{\mathcal{O}} = U_n \Sigma_n^{1/2}, \qquad \hat{\mathcal{C}}U_p = \Sigma_n^{1/2} V_n^T$$

since the 2-norms of $\hat{\mathcal{O}}$ and $\hat{\mathcal{C}}U_p$ are equal for this choice. An estimate of A_d may then be solved via the minimization

$$\hat{A}_d = \arg\min_{A_d} \left|\left| \hat{\mathcal{O}} A_d \hat{\mathcal{C}} U_p - \overline{\Omega} \right|\right|_F \tag{18}$$

in which F indicates the Frobenius norm. If no constraints are placed on $\hat{A}_d$, this has the analytical solution

$$\hat{A}_d = \hat{\mathcal{O}}^{\dagger} \overline{\Omega} (\hat{\mathcal{C}}U_p)^{\dagger} = \Sigma_n^{-1/2} U_n^T \overline{\Omega} V_n \Sigma_n^{-1/2}. \tag{19}$$

C_d may be then estimated from the top n_y rows of the extended observability matrix as

$$\hat{C}_d = \hat{\mathcal{O}}_{(1:n_y,:)} \tag{20}$$

where "MATLAB-style" indexing notation has been used in the subscript.

D. Model-Order Selection

Generally, n is not known beforehand. The error between Ω_n and Ω is, however, equal to the first singular value of Σ_s

$$\sigma_{n+1} = ||\Omega_n - \Omega||_2$$

and we can estimate n from the drop-off of the singular values of Ω due to (15) and the system-theoretic interpretation of the singular values of H. The reasoning behind this is as follows. The singular values of H correspond to the magnitudes of each element of the state vector $x_d(k)$ in an "internally balanced" state-basis. Consequently, the singular values of H can be interpreted as a set of gains for (10), and reducing the rank of H by truncating its singular values in the deterministic case is in fact a form of optimal model reduction. (Further discussions on the various meanings of the singular values of H can be found in the literature of robust control. See [18, Ch. 8].) Additionally, because the inverse of U_p is the bidiagonal matrix

$$U_p^{-1} = \begin{bmatrix} 1 & -1 & 0 & \\ 0 & 1 & -1 & \ddots \\ & \ddots & \ddots & \ddots \end{bmatrix}$$

it can be verified by inspection that

$$\left|\left|U_p^{-1}\right|\right|_1 = 2, \qquad \left|\left|U_p^{-1}\right|\right|_\infty = 2$$

where $||\cdot||_1$ is the induced 1-norm and $||\cdot||_\infty$ the induced ∞-norm. The maximum singular value of U_p^{-1} then has the upper bound [19, Fact 9.8.23]

$$\sigma_{\max}(U_p^{-1}) < \left(\left|\left|U_p^{-1}\right|\right|_1 \left|\left|U_p^{-1}\right|\right|_\infty\right)^{-1/2} = 2.$$

From the identity [19, Corollary 9.5.5]

$$\sigma_{\min}(U_p) = \left[\sigma_{\max}(U_p)\right]^{-1}$$

we have

$$\sigma_{\min}(U_p) > 1/2.$$

Finally, the identity [19, Proposition 9.6.4]

$$\sigma_i(H)\sigma_{\min}(U_p) \leq \sigma_i(HU_p)$$

leads to

$$\frac{1}{2}\sigma_i(H) < \sigma_i(HU_p)$$

and so the multiplication of H on the right by U_p will not reduce its singular values by more than half. Indeed, they may be increased.

Additionally, if the content of E in (15) is Gaussian, then the singular values of E are equal to the variance of the noise. If E is colored, then it can be represented as filtered white noise, and its singular values will be equal to the product of the noise variance and the system 2-norm of the noise filter [16]. For reasonable signal-to-noise ratios, the singular values of HU_p will be greater than those of E. Thus a suitable n can be chosen by examining the singular values of Ω and selecting a value of n for which $\sigma_n - \sigma_{n+1}$ is large.

E. Estimation of the Parameter B_d

At this point, an estimate $\hat{B}$ could be taken from the first column of $\hat{C}U_p$, but an improved estimate can be calculated by solving a linear least-squares problem, which will also allow the incorporation of constraints later. Given estimates $\hat{A}_d$ and $\hat{C}_d$ and N samples of a measured step response, let $\hat{B}_d$ be the solution of

$$\hat{B}_d = \arg\min_B ||\xi - \phi B||_2 \tag{21}$$

where

$$\xi = \begin{bmatrix} y_d(0) \\ y_d(1) \\ \vdots \\ y_d(N-1) \end{bmatrix}, \qquad \phi = \begin{bmatrix} \phi(0) \\ \phi(1) \\ \vdots \\ \phi(N-1) \end{bmatrix} \tag{22}$$

and

$$\phi(k) = \sum_{l=0}^{k-1} \hat{C}_d \hat{A}_d^{k-l-1}. \tag{23}$$

In the unconstrained case, this has the analytical solution

$$\hat{B}_d = \phi^\dagger \xi. \tag{24}$$

Note that N does not have to be equal to the number of samples used to construct the data matrices of (13). Thus, given a step response measurement $y_d(k)$, an estimate of the state-space parameters (A_d, B_d, C_d) may be found from (19), (20), and (24). Computing $\phi(k)$ directly from (23) is often the most computationally expensive step of the identification algorithm, but it can be very efficiently calculated as a specific state sequence of the dual system of (10). See [20] for details.

IV. Constraining the Estimate

When noise-free data is used, the SBR method gives an exact reconstruction of multioutput systems of (10) up to a change of state basis. Even in the case of noise-corrupted estimates, the method allows the model order to be selected during the identification process, and because the order of the model is equal to the rank of (12), the system is also guaranteed to be minimal, so that n cannot be reduced [10].

The model structure (10), however, allows a great deal more freedom than (1). If noise-corrupted measurements are used, the SBR method might not produce a model compatible with the step-response representation (1) unless additional constraints are in place. In the following section, we add semidefinite constraints to the parameters (A_d, B_d, C_d) to ensure that the identified model is consistent with (1).

Overlooked until recently is the fact that, although the original SBR estimate is solved analytically, the solution is the minimizer of a cost function that is strictly convex [21]. In fact, it is an affine parameterization inside a Frobenius norm, which may be transformed into a linear-programming cost function [22]. The convexity of this cost function allows the incorporation of convex constraints on the location of the poles of the estimate in the complex plane. These constraints are stated as LMIs. In our proposed method, we formulate LMIs that constrain the poles of a discrete-time system estimate to lie on the real number line between 0 and 1, which guarantees continuous-time poles that are real, stable, and may be realized in continuous time. This results in a semidefinite program which is solvable via linear programming interior point methods.

If (10) is the discretization of (1), then the assumptions of τ_i require constraints to be placed on the eigenvalues of A_d. These are stated in the following.

Proposition 1: System (10) is a discretization of (1) if and only if all eigenvalues $\lambda_d^{(i)}$ of A_d satisfy the following constraints:

$$|\lambda_d^{(i)}| < 1 \tag{25}$$

$$\mathrm{Im}(\lambda_d^{(i)}) = 0 \tag{26}$$

$$\mathrm{Re}(\lambda_d^{(i)}) > 0. \tag{27}$$

Proof: Noting that $\lambda_d^{(i)} = e^{-T_s/\tau_i}$, (25) and (26) follow directly from (2) and (3) $= 0$, respectively. Equation (27) is required so that the zero-order hold discretization formulas are invertible. ■

Thus in order for (10) to be converted to (1), (25)–(27), must be satisfied. The eigenvalues $\lambda_d^{(i)}$ are a nonlinear function of the entries of A_d, however, so a cost function that includes A_d cannot be minimized over a convex set if the eigenvalues are constrained directly. To translate the eigenvalue constraints into convex constrains on A_d, we introduce the concept of LMI regions, originally developed in [23].

A. LMI Regions

An LMI region is a convex region $\mathcal{D}$ of the complex plane, defined in terms of a symmetric matrix α and a square matrix β, as

$$\mathcal{D} = \{z \in \mathbb{C} : f_{\mathcal{D}}(z) \succeq 0\} \tag{28}$$

where

$$f_{\mathcal{D}}(z) = \alpha + \beta z + \beta^T \bar{z}. \tag{29}$$

We will call $f_{\mathcal{D}}(z)$ for a given $\mathcal{D}$ the describing function of $\mathcal{D}$. LMI regions generalize Lyapunov stability for continuous and discrete time systems. We repeat the central theorem of [23] here for future reference.

Theorem 1: The eigenvalues of a matrix A lie within an LMI region with describing function (29) if and only if there exists a matrix $P \in \mathbb{R}^{n\times n}$ such that

$$P = P^T \succ 0, \qquad \mathcal{M}_{\mathcal{D}}(A,\ P) \succeq 0 \tag{30}$$

in which

$$\mathcal{M}_{\mathcal{D}}(A,\ P) = \alpha \otimes P + \beta \otimes (AP) + \beta^T \otimes (AP)^T. \tag{31}$$

The original definition of an LMI region in [23] has $\prec$ in place of $\succeq$ for (28) and (30). We adopt the above definition instead so that our results are straightforward to implement as a semidefinite program and because the real axis cannot be parameterized as an LMI region if (28) uses a strict inequality.

The intersection of two LMI regions $\mathcal{D}_1$ and $\mathcal{D}_2$ is also an LMI region, described by the matrix function

$$f_{\mathcal{D}_1\cap\mathcal{D}_2}(z) = \begin{bmatrix} f_{\mathcal{D}_1}(z) & 0 \\ 0 & f_{\mathcal{D}_2}(z) \end{bmatrix}. \tag{32}$$

In general, the $(\alpha,\ \beta)$ pair that describes an LMI region is not unique.

The following three LMI regions correspond to the three constraints on $\lambda_d^{(i)}$ in (25)–(27). Each proposition may be proven by analytically solving for the eigenvalues of describing function.

The constraint $|\lambda_d^{(i)}| < 1$ is equivalent to saying $\lambda_d^{(i)}$ must lie within the unit circle. To provide some additional degree of stability for the identified models, we may constrain eigenvalues to the disc of radius $1 - \delta_s$.

Proposition 2 (Discrete-Time Stable Region): The set

$$\mathcal{S} = \{z \in \mathbb{C} : |z| \le 1 - \delta_s, \qquad 0 \le \delta_s \le 1\}$$

is equivalent to the LMI region $f_{\mathcal{S}}(z) \succeq 0$

$$f_{\mathcal{S}}(z) = (1-\delta_s)I_2 + \begin{bmatrix} 0 & 1 \\ 0 & 0 \end{bmatrix} z + \begin{bmatrix} 0 & 0 \\ 1 & 0 \end{bmatrix} \bar{z}. \tag{33}$$

If $\delta_s = 0$, this region applied with results in the standard discrete-time Lyapunov stability condition when applied with Theorem 1.

The real number line $\mathbb{R}$ is equivalent to the LMI region $f_{\mathbb{R}}(z) \succeq 0$

$$f_{\mathbb{R}}(z) = \begin{bmatrix} 0 & 1 \\ -1 & 0 \end{bmatrix} z + \begin{bmatrix} 0 & -1 \\ 1 & 0 \end{bmatrix} \bar{z}.$$

This constraint, however, uses two inequalities to define an equality, which can create problems for interior-point-based numerical solvers. Instead, we include a parameter to describe a small band around the real axis in the complex plane.

Proposition 3 (Constrained Imaginary Region): The set

$$\mathcal{R} = \{z \in \mathbb{C} : |\mathrm{Im}(z)| \le \delta_r, \quad \delta_r \ge 0\}$$

is equivalent to the LMI region $f_{\mathcal{R}}(z) \succeq 0$

$$f_{\mathcal{R}}(z) = 2\delta_r I_2 + \begin{bmatrix} 0 & 1 \\ -1 & 0 \end{bmatrix} z + \begin{bmatrix} 0 & -1 \\ 1 & 0 \end{bmatrix} \bar{z}. \tag{34}$$

The parameter δ_r can be made very small while still resulting in a numerically robust optimization. Any remaining imaginary part of z can then be truncated with a negligible effect on the response of the model.

If the eigenvalues of A_d are allowed to have negative real parts, then inverting a zero-order hold via the matrix logarithm will result in a complex-valued A_c. To guarantee that $\log(A_d)$ is real and unique, we construct an LMI region that describes the positive right-half plane. This region is also parameterized so that the region begins some distance away from the imaginary axis.

Proposition 4 (Positive Real Region): The set

$$\mathcal{P} = \{z \in \mathbb{C} : \mathrm{Re}(z) \ge \delta_p, \quad \delta_p \ge 0\}$$

is equivalent to the LMI region $f_{\mathcal{P}}(z) \succeq 0$

$$f_{\mathcal{P}}(z) = \delta_p \begin{bmatrix} 2 & 0 \\ 0 & -2 \end{bmatrix} + \begin{bmatrix} 0 & 0 \\ 0 & 1 \end{bmatrix} z + \begin{bmatrix} 0 & 0 \\ 0 & 1 \end{bmatrix} \bar{z}. \tag{35}$$

Combining Theorem 1 with (32), we formulate an LMI region to satisfy all three constraints on $\lambda_d^{(i)}$ and state the following Lyapunov-type condition for $\lambda_d^{(i)}$, which may be incorporated into a convex optimization program. A diagram of the LMI region is shown in Fig. 1.

Corollary 1: The discrete-time state-space model (10) is the discretization of a continuous-time model (1) if and only if there exists a matrix $P \in \mathbb{R}^{n\times n}$ such that

$$P = P^T \succ 0, \qquad \mathcal{M}_d(A_d,\ P) \succeq 0$$

in which

$$\begin{aligned} \mathcal{M}_d(A_d,\ P) &= \alpha_d \otimes P + \beta_d \otimes (A_d P) + \beta^T \otimes (A_d P)^T \\ \alpha_d &= \begin{bmatrix} (1-\delta_s)I_2 & 0 & 0 \\ 0 & 2\delta_r I & 0 \\ 0 & 0 & 2\delta_p I_2 \end{bmatrix} \\ \beta_d &= \begin{bmatrix} 0 & 1 & 0 & 0 & 0 & 0 \\ 0 & 0 & 0 & 0 & 0 & 0 \\ 0 & 0 & 0 & 1 & 0 & 0 \\ 0 & 0 & -1 & 0 & 0 & 0 \\ 0 & 0 & 0 & 0 & 0 & 0 \\ 0 & 0 & 0 & 0 & 0 & 1 \end{bmatrix} \end{aligned} \tag{36}$$

with $\delta_s = \delta_r = \delta_p = 0$.

The corollary results in sufficient conditions for A_d for any $\delta_s,\ \delta_p \in [0,\ 1)$, and we may still use a nonzero δ_r, provided any remaining imaginary components of $\lambda_d^{(i)}$ are neglected. In practice, δ_r can be very small so that the imaginary components are near machine precision.

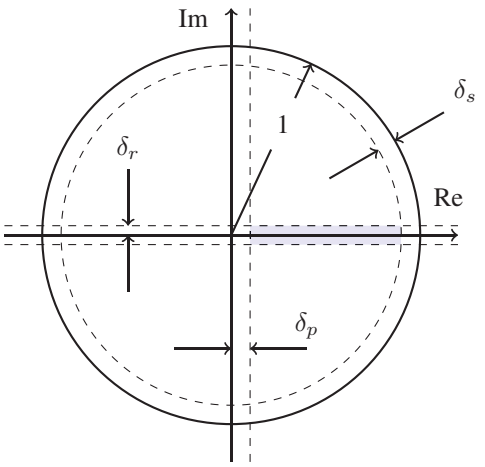

Fig. 1. LMI region used for identification. Poles of the system estimate are constrained to the shaded region.

B. Additional Constraints on the Discrete-Time State-Space Parameters

Additional assumptions may be made regarding (1), such as the assumption that steady-state value of the step-response is equal to some value determined from prior knowledge. For example, if the ambient temperature or steady-state behavior of the system is known with high precision, then the value of the sum of R_i can be assumed beforehand.

Suppose $y(\infty)$ is the steady-state value of (1). Because the continuous- and discrete-time systems have the same steady-state value, we may form the following constraint.

Proposition 5: If (1) satisfies

$$\sum_{i=1}^{n} R_i = y(\infty) \tag{37}$$

then (10) is a discretization of (1) if and only if

$$C_d \left(I - A_d\right)^{-1} B_d = y(\infty). \tag{38}$$

In thermal analysis, it is generally required that the transient thermal response to a step change be monotonically increasing. It is therefore necessary that its discretization also be monotonically increasing, and so the difference between one time step ahead and the current time step must be positive. From the discrete-time step response (11), this may be stated as the following inequality constraint.

Proposition 6: If $y(t)$ in (1) is monotonically increasing, then (10) is a discretization of (1) only if

$$C_d A_d^k B_d > 0 \qquad \forall\, k. \tag{39}$$

At times, it is possible to assume that all R_i in (1) are positive. This may also be translated into a constraint on the discrete-time state-space model.

Proposition 7: If (1) satisfies

$$R_i > 0$$

then (10) is a discretization of (1) if and only if:

1) A_d satisfies (26) and (27):

2)
$$\left(\Lambda_c^{-1} \otimes C_d\right) \begin{bmatrix} M_c^{(1)} \\ M_c^{(2)} \\ \vdots \\ M_c^{(n)} \end{bmatrix} \left(A_d - I\right)^{-1} A_c B_d > 0 \tag{40}$$

where (using the matrix logarithm)

$$A_c = \frac{1}{T_s} \log(A_d). \tag{41}$$

$A_c = V_c \Lambda_c V_c^{-1}$ is the eigenvalue decomposition, $M_c^{(i)}$ is given by (9), and $\otimes$ is the Kronecker product.

Proof: From (8), we know that R_i are real if and only if $\mathrm{Im}(\lambda_d^{(i)}) = 0$. Also, (41) exists if and only if $\mathrm{Re}(\lambda_i^{(i)}) > 0$. Then using (8), (40) reduces to

$$\begin{bmatrix} R_1 \\ R_2 \\ \vdots \\ R_n \end{bmatrix} > 0$$

which is the required constraint. ■

It should be emphasized, however, that these constraints are independent of the eigenvalue constraints and do not need to be included if the experimenter desires a model with a step response that is not strictly monotonically increasing.

C. Incorporating Constraints into the SBR Method

The LMI constraint (36) is convex since it is linear in A_d, and if we have estimates of A_d and C_d, then (38)–(40) are also convex since they are linear in B_d. Thus if a convex minimization of A_d and C_d is followed by a convex minimization of B_d, the full problem may be stated as a convex optimization which guarantees that the resulting estimate is a discretization of (1). The SBR method, introduced in the previous section, provides just such a sequence of optimizations.

Though (18) is convex in A_d, the general constraint form (31) contains the product $A_d P$. We therefore modify (18) to also contain the product $A_d P$. Let $W_r = (\hat{\mathcal{O}} U_p)^{\dagger} P$ be a right-hand weighting matrix to form the augmented cost function

$$\begin{aligned} J'(A,\ P) &= \left|\left| \hat{\mathcal{O}} A_d \hat{\mathcal{C}} U_p W_r - \overline{\Omega} W_r \right|\right|_F \\ &= \left|\left| \hat{\mathcal{O}} A_d P - \overline{\Omega} (\hat{\mathcal{C}} U_p)^{\dagger} P \right|\right|_F . \end{aligned} \tag{42}$$

Note that the unconstrained minimizer of (42) is still given by (19), regardless of the value of P. This is not necessarily true, however, when A_d is constrained to be within an arbitrary convex set, unless $P = I$. To reduce any errors this may cause, as well as to increase the numerical stability of the problem, we provide as a constraint

$$\mathrm{trace}(P) = n$$

which still allows for the possibility of $P = I$ while not overconstraining the problem.

We still must reparameterize (42) to be affine in the parameters in order to formulate the constrained optimization as a

convex optimization. Letting $Q = A_d P$, we form the following convex optimization problem with convex constraints.

Given estimates $\hat{\mathcal{O}}$, $\hat{\mathcal{C}}U_p$, and $\overline{\mathbf{\Omega}}$

$$\begin{aligned} \min \quad & J(Q,\ P) \\ \text{s.t.} \quad & \mathcal{M}(Q,\ P) \succeq 0 \\ & P = P^T \succ 0 \\ & \operatorname{trace}(P) = n \end{aligned} \tag{43}$$

in which

$$J(Q,\ P) = \left|\left|\hat{\mathcal{O}}_0 Q - \overline{\mathbf{\Omega}}(\hat{\mathcal{C}}U_p)^{\dagger} P\right|\right|_F$$

and

$$\mathcal{M}(Q,\ P) = \alpha_d \otimes P + \beta_d \otimes Q + \beta^T \otimes Q^T.$$

This is equivalent to a linear program with mixed equality, quadratic, and semidefinite constraints [24]. Once Q and P are solved for, let $\hat{A}_d = QP^{-1}$. With $\hat{C}_d$ taken from (20), (38)–(40) are linear in $\hat{B}_d$ and can be incorporated into (21), forming a second convex optimization problem with convex constraints.

Given ξ and ϕ from (22)

$$\begin{aligned} \min \quad & \left|\left|\xi - \phi \hat{B}_d\right|\right|_2 \\ \text{(optionally) s.t.} \quad & (38) - (40). \end{aligned} \tag{44}$$

Thus by solving two convex optimization problems, an estimate of a discrete-time state-space system (10) which is guaranteed to be a discretization of a model of (1) is found.

V. Application to the Thermal Response of an LED

To demonstrate its effectiveness, the proposed algorithm was applied to the measured thermal response of a Cree XLamp XP-E LED [25].

A. Experimental Setup

The junction temperature of the device was measured indirectly as recommended in the Electronic Industries Association specification EIA/JEDEC JESD51-1. In the specification, junction temperature is assumed to be proportional to the forward voltage. The scaling between junction temperature and forward voltage, or K-factor, was determined by first driving the forward voltage above the diode's cut-in voltage using a measurement current low enough so as not to induce significant self-heating. The K-factor was then be found by adjusting the temperature of the device and measuring the forward voltage. For these experiments, the LED was driven by a Vektrex SpikeSafe current source, voltages were measured with an Agilent 34411A digital multimeter, and temperature was controlled by a prototype Vektrex Thermal Platform Controller. A schematic of the experimental configuration can be seen in Fig. 2.

A 600-mA step was applied to the LED and 2 s of the step response was measured at 50 kHz. The measured change in forward voltage was approximately 2.6 V. A plot of the measured voltage after conversion to temperature can be seen in Fig. 4.

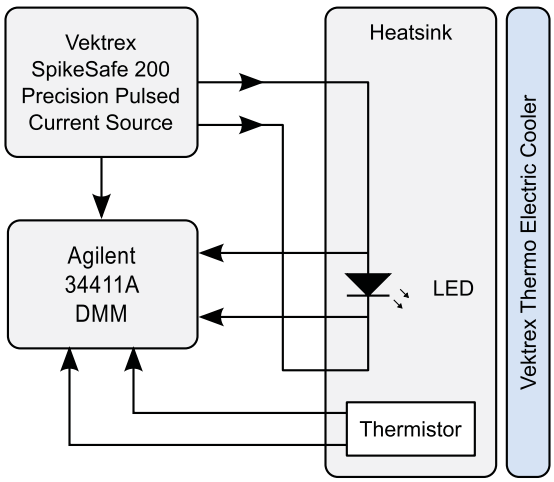

Fig. 2. Experimental setup for thermal step-response measurements.

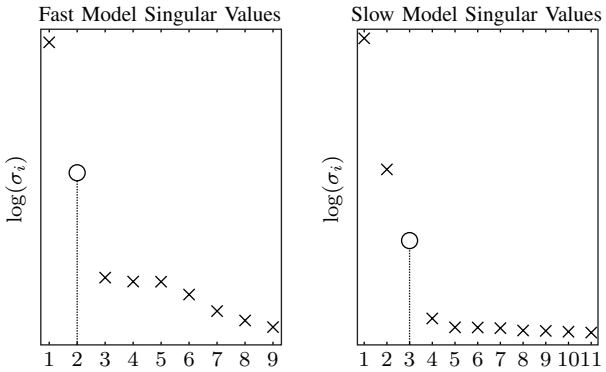

Fig. 3. Singular values of (16) for fast and slow datasets. The chosen model order for each is marked by ∘. The scale of the y-axis is arbitrary and was intentionally omitted.

B. Analysis of the Response

The data was analyzed in MATLAB using the method described above.[1] Because the system itself contains both fast and slow dynamics, the system is "stiff" in the sense that the underlying differential equations are ill-conditioned. Thus to keep the identification procedure computationally feasible, two models were identified. The first was a "fast" model identified from 0 to 0.002 s (the first 100 samples of data). The fast-model estimate was not sensitive to the number of samples used so long as the end of the fast response was chosen to be in a region of the response where the slope of the log-time plot was fairly constant (see Fig. 4). The number of block-rows for the data matrices was chosen to be 9.

The second model was a "slow" model identified from a dataset downsampled by a factor of 1000. Before downsampling, the data was filtered forward and backward through a fourth-order Butterworth filter with a cutoff frequency of 0.1 rad/s. The number of block rows for these data matrices was chosen to be 11.

Singular values of (16) for each dataset are shown in Fig. 3. For each, there is a sharp drop off in magnitude

[1] As of publication, MATLAB software for identifying constrained models can be found at http://sites.google.com/site/dnmiller/.

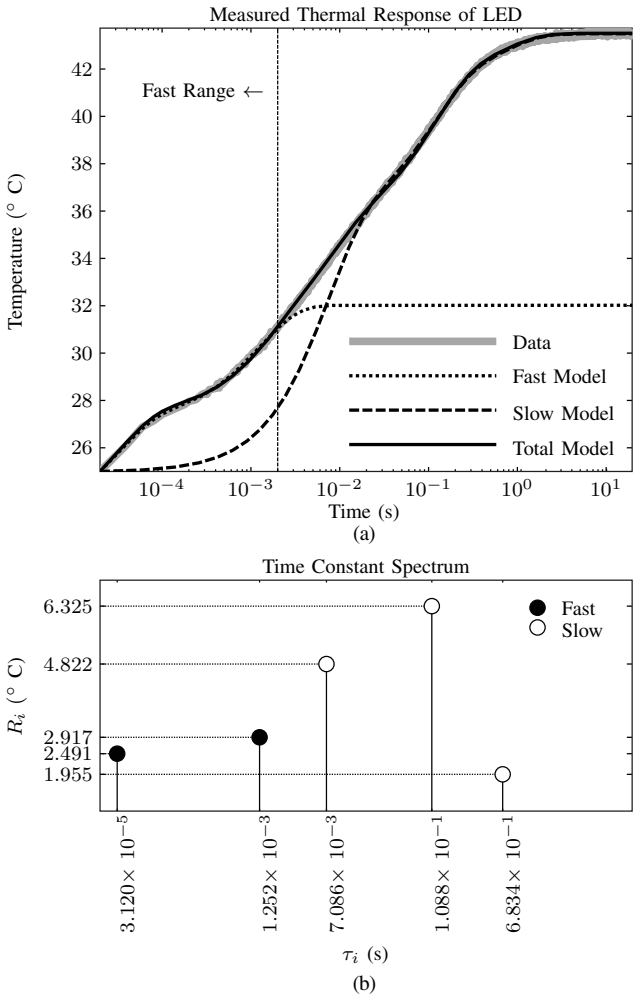

Fig. 4. (a) Simulations of fast, slow, and total models together with measured data. (b) Time-constant spectrum, with constants from fast and slow models. The x-axes on both plots are equal. A line in the time plot denotes where the domain of the fast model ends.

within the first few singular values. This implies the order of the underlying dynamics. It also suggests that increasing the model order any higher would not significantly reduce the error between the data and the model. Additionally, increasing the model order would result in $(R_i,\ \tau_i)$ pairs that show signs of linear dependence on one another, so that the number of time constants would not be minimal.

Estimates of $\hat{A}_d$ and $\hat{C}_d$ were found for fast and slow models by solving (43) with YALMIP [26] using SDPT3 [27] as the selected solver. $\hat{B}_d$ was solved for each model using the unconstrained solution in (24). Note that these estimates of B_d are only used to simulate the fast and slow models and are not used to construct the final model. Simulations of both models together with raw data are shown in Fig. 4.

To combine the two models into one, the sampling time of the slow model was adjusted to match the fast model, and the total model A_d and C_d were taken to be

$$A_d^{(\text{total})} = \begin{bmatrix} A_d^{(\text{fast})} & 0 \\ 0 & A_d^{(\text{slow})} \end{bmatrix}, \qquad C_d^{(\text{total})} = \begin{bmatrix} C_d^{(\text{fast})} \\ C_d^{(\text{slow})} \end{bmatrix}.$$

$B_d^{(\text{total})}$ was found by solving (44) with (38) and (39). To avoid calculating to product of $C_d^{(\text{total})}$ and $\left[A_d^{(\text{total})}\right]^k$ for $k = 0$ to $k = 980\,000$, 150 values of k spaced logarithmically along the time axis were chosen. Of these calculated products, 101 had very small magnitudes (less than 0.01) and were not used for the regressor for calculating $B_d^{(\text{total})}$. The steady-state value $y(\infty)$ was constrained to be the average of the last 400 000 samples. For (39), 150 values of $C_d A_d^k$ were calculated corresponding to the 150 data points. Of the 150 calculated values of $C_d A_d^k$, 101 had very small magnitudes and were discarded. Values of $C_d A_d^k$ which had an entry of magnitude less than 0.01 were discarded to prevent numerical issues, resulting in 49 total inequality constraints of (39).

A simulation of the total model is shown in Fig. 4. The time-constant spectrum of the model is shown underneath. Of note is that the entire model is described by only 10 parameters and required no nonlinear optimization.

VI. Conclusion

We presented a new method for the identification of thermal responses of semiconductor devices that used a realization-based procedure with a fixed number of linear algebraic operations combined with convex optimization methods. The method guarantees real and stable solutions for the time constants and their relative contributions, and may optionally include constraints to fix the steady-state value of the response, i.e., the total contribution of the time constants, as well as positivity of the time-constant contributions.

Because the numerical procedure is based on a fixed number of linear algebraic operations and convex optimization techniques, solutions for the time constants and their contributions are guaranteed to be found. Changes in the values of R_i and τ_i, such as those shown in Fig. 4, allow the detection of physical changes in thermal resistance of the elements of the system. Additionally, changes in the singular values, such as those shown in Fig. 3, can be used to detect for change in the model order, which would indicate the presence of additional time delay in the response. This makes the method particularly well suited for defect detection in semiconductor devices.

References

[1] V. Székely and T. Van Bien, "Fine structure of heat flow path in semiconductor devices: A measurement and identification method," *Solid-State Electron.*, vol. 31, no. 9, pp. 1363–1368, 1988.

[2] V. Székely, "On the representation of infinite-length distributed RC one-ports," *IEEE Trans. Circuits Syst.*, vol. 38, no. 7, pp. 711–719, Jul. 1991.

[3] V. Székely and M. Rencz, "Thermal dynamics and the time constant domain," *IEEE Trans. Compon. Packag. Technol.*, vol. 23, no. 3, pp. 587–594, Sep. 2000.

[4] V. Székely, "A new evaluation method of thermal transient measurement results," *Microelectron. J.*, vol. 28, no. 3, pp. 277–292, 1997.

[5] V. Székely, "Identification of RC networks by deconvolution: Chances and limits," *IEEE Trans. Circuits Syst.*, vol. 45, no. 3, pp. 244–258, Mar. 1998.

[6] M. Rencz, A. Poppe, E. Kollár, S. Ress, and V. Székely, "Increasing the accuracy of structure function based thermal material parameter measurements," *IEEE Trans. Compon. Packag. Technol.*, vol. 28, no. 1, pp. 51–57, Mar. 2005.

[7] J. Palacín, M. Salleras, J. Samitier, and S. Marco, "Dynamic compact thermal models with multiple power sources: Application to an ultrathin chip stacking technology," *IEEE Trans. Adv. Packag.*, vol. 28, no. 4, pp. 694–703, Nov. 2005.

[8] J. Palacín, M. Salleras, M. Puig, J. Samitier, and S. Marco, "Evolutionary algorithms for compact thermal modelling of microsystems: Application to a micro-pyrotechnic actuator," *J. Micromech. Microeng.*, vol. 14, no. 7, pp. 1074–1082, Jul. 2004.

[9] T. Bechtold, E. B. Rudnyi, and J. G. Korvink, "Automatic generation of compact electro-thermal models for semiconductor devices," *IEICE Trans. Electron.*, vol. E86-C, no. 3, pp. 459–465, 2003.

[10] B. L. Ho and R. E. Kalman, "Effective construction of linear state-variable models from input/output functions," *Regelungstechnik*, vol. 14, no. 12, pp. 545–548, 1966.

[11] P. H. Zeiger and J. A. McEwen, "Approximate linear realizations of given dimension via Ho's algorithm," *IEEE Trans. Autom. Control*, vol. 19, no. 2, p. 153, Apr. 1973.

[12] S.-Y. Kung, "A new identification and model reduction algorithm via singular value decomposition," in *Proc. 12th Asilomar Conf. Circuits, Syst., Comput.*, 1978, pp. 705–714.

[13] S.-Y. Kung and D. W. Lin, "Optimal Hankel-norm model reductions: Multivariable systems," *IEEE Trans. Autom. Control*, vol. 26, no. 4, pp. 832–852, Aug. 1981.

[14] J. van Helmont, A. van der Weiden, and H. Anneveld, "Design of optimal controller for a coal fired Benson boiler based on a modified approximate realisation algorithm," in *Applications of Multivariable System Techniques*, R. Whalley, Ed. Amsterdam, The Netherlands: Elsevier, 1990, pp. 313–320.

[15] D. N. Miller and R. A. de Callafon, "Subspace identification from classical realization methods," in *Proc. 15th IFAC Symp. Syst. Identificat.*, Saint-Malo, France, Jul. 2009, pp. 102–107.

[16] M. Verhaegen and V. Verdult, *Filtering and System Identification: A Least Squares Approach*, 1st ed. New York: Cambridge Univ. Press, May 2007.

[17] G. Golub and C. Van Loan, *Matrix Computations*, 3rd ed. Baltimore, MD: The Johns Hopkins Univ. Press, 1996.

[18] K. Zhou, J. C. Doyle, and K. Glover, *Robust and Optimal Control*. Englewood Cliffs, NJ: Prentice-Hall, Aug. 1995.

[19] D. S. Bernstein, *Matrix Mathematics: Theory, Facts, and Formulas*, 2nd ed. Princeton, NJ: Princeton Univ. Press, Jul. 2009.

[20] D. N. Miller and R. A. de Callafon, "Efficient identification of input dynamics for correlation function-based subspace identification," in *Proc. 18th IFAC World Congr.*, 2011, pp. 6511–6516.

[21] D. N. Miller and R. A. de Callafon, "Identification of linear time-invariant systems via constrained step-based realization," in *Proc. 16th IFAC Symp. Syst. Identificat.*, 2012.

[22] S. P. Boyd and L. Vandenberghe, *Convex Optimization*. Cambridge, U.K.: Cambridge Univ. Press, 2004.

[23] M. Chilali and P. Gahinet, "H_∞ design with pole placement constraints: An LMI approach," *IEEE Trans. Autom. Control*, vol. 41, no. 3, pp. 358–367, Mar. 1996.

[24] S. L. Lacy and D. S. Bernstein, "Subspace identification with guaranteed stability using constrained optimization," *IEEE Trans. Autom. Control*, vol. 48, no. 7, pp. 1259–1263, Jul. 2003.

[25] "Cree Â XLamp Â XP-E LEDs," Cree, Durham, NC, Tech. Rep. CLD-DS18.005, 2009.

[26] J. Löfberg, "YALMIP: A toolbox for modeling and optimization in MATLAB," in *Proc. IEEE Int. Symp. Comput.-Aided Control Syst. Design*, Apr. 2004, pp. 284–289.

[27] K.-C. Toh, M. J. Todd, and R. H. Tutuncu, "SDPT3—A MATLAB software package for semidefinite programming, version 1.3," *Optim. Methods Softw.*, vol. 11, nos. 1–4, pp. 545–581, 1999.

Daniel N. Miller (S'07) received the B.S. degree from the University of California, San Diego, in 2005, and the Ph.D. degree from the Jacobs School of Engineering, University of California, San Diego, in 2012, both in mechanical engineering.

He began his Ph.D. studies in 2009 after several years working in the aerospace industry with General Atomics Aeronautical Systems. He is currently with Vigilent Corporation, El Cerrito, CA, developing intelligent energy management systems for data centers. He is a fellow of the Gordon Center for Engineering Leadership and a former Air Force Research Laboratories Space Scholar. His current research interests include data-based experimental modeling techniques and robust control systems design.

Jeff Hulett received the B.S.E.E. degree from the Illinois Institute of Technology, IL.

He is a CTO of Vektrex, San Diego, CA. He has been active in the LED testing and reliability field since 2004. Prior to that, he led teams that designed numerous computer based products, including image processing systems, a space-qualified navigation computer for Japans H2A rocket, graphics accelerators for Indias air traffic control network, and high voltage programmable power sources for gene sequencing.

Mr. Hulett is a member of the Illumination Engineering Society of North America (IESNA) and he chairs the IESNA LM-80 working group that is focused on LED flux maintenance testing.

James McLaughlin received the B.S.E.E. degree from San Diego State University in 2008.

He is an electrical engineer at Vektrex, San Diego, CA. He has worked on many different projects at Vektrex, including embedded software development for Vektrex current sources, developing and maintaining procedures for photometric testing of LEDs, and developing and testing thermal resistance measurement procedures for LEDs, among many others. He plans to obtain an M.S.E.E. with a focus on digital signal processing, specifically applied to embedded systems for audio electronics.

Raymond A. de Callafon (M'12) received the M.Sc. and Ph.D. degrees in mechanical engineering from the Delft University of Technology, Delft, The Netherlands, in 1992 and 1998, respectively.

He is a Professor with the Department of Mechanical and Aerospace Engineering (MAE), University of California, San Diego. Since 1998, he has been with the Department of MAE. He is currently directing the System Identification and Control Laboratory and is a Faculty of the Center for Magnetic Recording Research (CMRR) directing the CMRR Servo Laboratory. His current research interests include experiment-based approximation modeling, control relevant system identification, and recursive/adaptive control.